Conditional Simulation of Spatially Variable Motions on 2D Grid

Timothy D. Ancheta
Lead Modeler, Risk Management Solutions, Inc., Newark, CA, USA

Jonathan P. Stewart
Professor and Chair, Dept. of Civil Engineering, University of California, Los Angeles, USA

ABSTRACT: Conditional simulation of spatially variable earthquake ground motion is required to incorporate kinematic interaction effects within response history analysis of structures. We present an approach that takes as input a seed motion and models for Fourier amplitude and phase variability that are functions of frequency and separation distance. The conditional simulation outputs are ground motions modified from the seed on a 2D grid having appropriate non-stationary characteristics while maintaining compatibility with the amplitude and phase variability models. The method applies the Fourier Integral Method to simulate random fields and extends short time Fourier transform analysis and synthesis to account for time and frequency nonstationary characteristics of earthquake time series.

We introduce a method to generate 1D, 2D, or even 3D fields of spatially variable ground motions (SVGM) conditioned on one or more input seed motions. Our approach merges short-time Fourier transform (STFT) analysis and synthesis (Allen and Rabiner, 1977) for non-stationary time series with the Fourier Integral Method (FIM) (Pardo-Iguzquiza and Chica-Olmo, 1993) for generating spatially correlated random fields. Issues addressed in the development of the method include selection of appropriate analysis and synthesis windows, selection of appropriate time-frequency bands, providing adequate scaling and zero padding of windows to ensure time domain weighting of unity, and translation of user-specified Fourier amplitude and phase variability models into covariance functions.

The proposed procedure overcomes limitations of previous conditional simulation methods. Methods proposed by Hao et al. (1989), Vanmarcke and Fenton (1991) and Vanmarcke et al. (1993) do not model Fourier amplitude and phase variability separately. The Abrahamson (1992a) method requires a penalty function to ensure a match to the target coherency function as it assumed the incorrect probability density function for the random phase and a high pass filter to remove high frequency noise incorporated during improper short time segment synthesis. The method describe here can model both components of SVGM separately, match the target correlation structures with a single step, and incorporate the non-stationary character of the ground motion without post processing. These improvements come with computation cost and a restriction on simulation locations to a uniformly space grid.

The following sections describe components of SVGM, introduce the proposed method, provide a simulation example, and discuss further development requirements.

1. COMPONENTS OF SVGM

In the absence of substantial changes in site condition across an observation (or application) region, SVGMs in the context of this paper include stochastic and deterministic components. The deterministic (or constant in space and time) component is called the wave passage effect, which is expressed as time delays in wave arrivals due to inclined vertically propagating plane waves or horizontally propagating surface waves. Wave passage introduces a shift in the Fourier phase (or delay in time) dependent on the

wave speed and the separation distance between locations. Stochastic variations of Fourier amplitude and phase unrelated to wave passage occur due to wave scattering and interference along the source-to-site ray paths. Random variations in the Fourier phase are represented through lagged coherency functions (e.g., Harichandran and Vanmarcke, 1986; Luco and Wong, 1986; Abrahamson, 1992b, Ancheta et al., 2011). Random variations of Fourier amplitudes are represented with standard deviation functions derived from Fourier amplitude differences (Abrahamson, 1992b, 2005; Ancheta et al., 2011).

Random variations of the wave passage effect are called arrival time perturbations by Zerva and Zervas (2002) and are caused by horizontal variations in the geologic structure encountered along the seismic ray paths. Arrival time perturbations can be measured as time differences from the expected and actual time delay (essentially, taking time delay as a random variable with deterministic mean and data-derived standard deviation) (Boissieres and Vanmarcke, 1995; Ancheta et al., 2011). Alternatively, both sources of random phase variations may be represented together in plane wave coherency (Abrahamson, 1992b).

2. CONDITIONAL SIMULATION OF GROUND MOTION

We represent earthquake ground motions in a space-time field as a combination of coherent signals plus noise. Two cases of conditional simulation are considered: when given a single time series as the seed motion or when given time series at all simulation locations. When given a single time series, the simulation creates the coherent and noise signal at all simulated locations. For the later case, the coherent and noise signal is given and the simulation must create a new instance of the space-time field by adding a new noise field. For the case that the original noise field does not match the selected SVGM functions, the simulation will create a matching field. Only the first case (single seed) is considered here.

The stationary (entire time series) notation is introduced first followed by the non-stationary (short time series) notation. We denote $a(\vec{r}, t)$ as a ground motion field recorded at the surface that consists of a coherent signal (represented by a sum of sinusoids) and noise. This field can be represented as:

$$a(\vec{r}, t) = \sum_n R_n(\vec{r}, t) cos[\theta_n(\vec{r}, t)] + e(\vec{r}, t) \quad (1)$$

where $R_n(\vec{r}, t)$ and $\theta_n(\vec{r}, t)$ are the amplitude and phase of the nth sinusoid at location $\vec{r}$ and time t, while $e(\vec{r}, t)$ is noise at location $\vec{r}$ and time t. Using X and E as the Fourier transform of the coherent and noise signals, we separate the contributions of various SVGM sources. Eqs. (2) and (3) show the Fourier amplitude and phase components of the signal and noise between two locations k and l for all frequencies considered,

$$a_k(t) = X_k\left(e^{j\omega_n t}\right) + E_{kl}\left(e^{j\omega_n t}\right) \quad (2)$$

$$a_k(t) = R_{X,k} e^{j\theta_{X,k}}\left(e^{j\omega_n t}\right) + R_{E,kl} e^{j\theta_{E,kl}}\left(e^{j\omega_n t}\right) \quad (3)$$

where ω_n is the frequency at index n, $R_{X,k}$ and $\theta_{X,k}$ is the coherent signal Fourier amplitude and phase at location k, $R_{E,kl}$ and $\theta_{E,kl}$ is the noise of the Fourier amplitude and phase between location k and l. The noise components represent the stochastic sources discussed in Section 1. The statistics of the noise Fourier amplitude and phase between earthquake recordings is described by Ancheta et al. (2011), which enables both to be modeled as Gaussian random numbers. The model for the Gaussian random numbers is described in Sections 3.1-3.2.

The stochastic spectral modifications in Eq. (2) and (3) assume a stationary time series. However, earthquake ground motions are non-stationary because of the sequencing of P-, S-, and surface waves having different frequency contents. The stationary signal and noise Fourier components can be replaced with their short-time Fourier transforms (Allen and Rabiner, 1977; Serra and Smith, 1990):

$$X_{m,k}\left(e^{j\omega_n}\right) = \sum_{t=0}^{T-1} w(t)\, a_k(t + mH)e^{-j\omega t} \quad (4)$$

$$E_{m,kl}\left(e^{j\omega_n}\right) = \sum_{t=0}^{T-1} w(t)\, e_{kl}(t + mH)e^{-j\omega_n t} \quad (5)$$

where $w(t)$ is the window that selectively determines and weights the portion of $a_k(t)$ being analyzed, t is the time index within the window, m is the index of the segment, and H is the hop size or number of time increments between segments. Suitable windows, hop size, and criteria for window selection are discussed in Section 4. The window width or as per Allen and Rabiner (1977) window duration, T, are discussed within this section.

The STFT calculation is the analysis phase. The synthesis phase combines the STFTs to recreate a time series. The consequence of the two stages on the selected window is discussed in Section 4. The synthesis method selected is called Overlap Addition (Allen and Rabiner, 1977). Overlap addition between the signal and noise is computed as:

$$a_l(t) = \sum_m \sum_n \left(X_{m,k}(e^{j\omega_n}) + E_{m,kl}(e^{j\omega_n}) \right) e^{j\omega_n t} \quad (6)$$

where the STFT consisting of the signal plus noise is first inversed to form a number of short time segments. Depending on the window selected in Eqs. (4) and (5) the short time segments may or may not overlap but are aligned by their individual absolute start times and summed.

We alter the STFT analysis and Overlap Addition synthesis from Allen and Rabiner (1977) to account for the non-stationarity of earthquake ground motions. Whereas Eq (6) uses a single segment width, T, we allow for multiple segment widths as follows:

$$a_l(t) =$$
$$\sum_f \sum_m \sum_{n\_lower}^{n\_upper} \left(X_{f,m,k}(e^{j\omega_n}) + E_{f,m,kl}(e^{j\omega_n}) \right) e^{j\omega_n t} \quad (7)$$

where f is the index for the different segment widths used and n_lower and n_upper are the upper and lower frequency indices associated with each segment width. The frequencies between the upper and lower indices are modified with the addition of the noise component while frequencies outside are not. The use of the multiple segment widths is motivated by different frequency bands being

approximately stationary over different window lengths. For example, a low frequency or large wavelength ground motion will be stationary over a long duration or long segment width. A high frequency or short wavelength ground motion will be stationary over a short duration. Therefore, each segment width is associated with a frequency band for which the Fourier components are assumed to be stationary. Table 1 give example pairings of segment durations and frequency bands.

The number of segment durations used will determine the number of time series created with Eq. (7). To create a single time series in which ground motion components at all frequencies are modified, the modified time series from Eq. (7) are transformed into the frequency domain and combined. Only the modified frequencies of each time series are combined to create a full modified spectra. The modified spectra are inversed into the time domain to create a single time series with the full frequency range modified.

Table 1: *Segment duration and frequency bands used in the Abrahamson (1992a) routine. T is the duration of the seed series.*

Segment Duration, L_i (sec)	Freq. limits, b_i (Hz)
1.28	2-Nyquist
2.56	1-2
5.12	0.5-1
10.24	0.25-0.5
20.48	0.12-0.25
T	0-0.12

Now expanding back out to the 2D plane (field) for which ground motions are to be simulated, the signal plus noise at simulation locations can be constructed with Eq 7 using a random field instead of single random number for the noise Fourier amplitude and phase. The random field for the amplitude and phase are created independently using the Fourier Integral

Method (FIM) (Pardo-Iguzquiza and Chica-Olmo, 1993), as discussed in Section 6.

3. STOCHASTIC AMPLITUDE AND PHASE

3.1. Phase

Stochastic phase has two components: stochastic phase unrelated to the wave passage effect and arrival time perturbations. This section only discusses the statistics of the stochastic phase for the generation of the random phase component of the noise in Eq. (3). The stochastic phase determined by Ancheta et al. (2011) can be modeled as Gaussian with a standard deviation, $\sigma_\theta(\omega_n, \xi)$, as a function of frequency and separation distance, ξ, between two locations. However, stochastic phase is modeled with coherency functions rather than functions directly describing the phase differences. Coherency is the measure of similarity between two time series. Lagged coherency is defined as the amplitude of coherency while plane wave coherency is defined as the real value of coherency when the time series are aligned using a single wave speed. A more complete definition of coherency, plane wave, and lagged coherency can be found in Abrahamson (1992b).

As coherency functions cannot be used in the forward simulation of random phase a coherency function is translated into a power spectral density matrix by Hao et al. (1989) or into a scale factor (α) representing the fraction of the Fourier phase that is deterministic by Abrahamson (1992b). Alternatively a coherency function may be translated into an equivalent standard deviation of phase, $\sigma_\theta(\omega_n, \xi)$ (Ancheta, 2010):

$$E[\gamma_{pw}(\omega_n, \xi)] = E[|\gamma|(\omega_n, \xi)] = e^{\left(-0.5\sigma_\theta^2(\omega_n, \xi)\right)} \quad (8)$$

When $\sigma_\theta(\omega_n, \xi)$ is related to plane wave coherency, $\gamma_{pw}(\omega_n, \xi)$, arrival time perturbations and the stochastic phase are combined. When $\sigma_\theta(\omega_n, \xi)$ is related to lagged coherency, $|\gamma|(\omega_n, \xi)$, arrival time perturbations must be added separately. The wave passage effect is not discussed further in this paper.

To create simulations over a 2D grid using the Fourier Integral Method, a coherency function must be translated into a covariance function. The covariance function, $C_\theta(\omega_n, \xi)$, for the stochastic phase is simply the variance between Fourier phase differences binned by separation distance (or lag). Beginning with the relationship between coherency and $\sigma_\theta(\omega_n, \xi)$ from Eq. (8), the covariance function can be created by isolating σ_θ^2 as follows:

$$ln\left(E[\gamma_{pw}(\omega_n, \xi)]\right) = ln\left(e^{\left(-0.5\sigma_\theta^2(\omega_n, \xi)\right)}\right) \quad (9)$$

$$ln\left(E[\gamma_{pw}(\omega_n, \xi)]\right) = -0.5\sigma_\theta^2(\omega_n, \xi) \quad (10)$$

$$C_\theta(\omega_n, \xi) = -2ln\left(E[\gamma_{pw}(\omega_n, \xi)]\right) \quad (11)$$

The covariance function above is strongly frequency-dependent. Figure 1 shows example covariance functions for various frequencies.
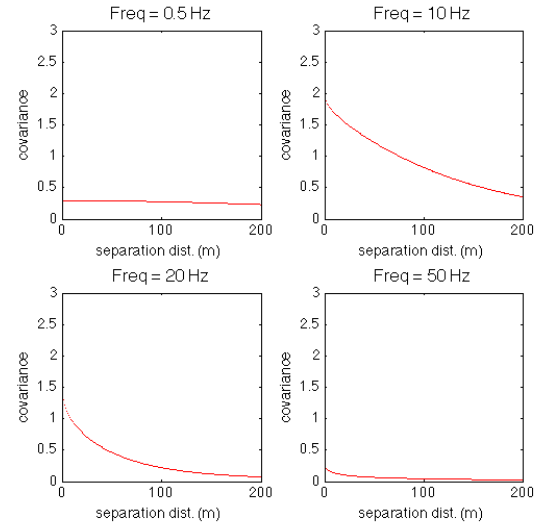

Figure 1: Covariance functions derived from lagged coherency model by Ancheta et al. (2011).

3.2. Amplitude

Stochastic amplitude has been studied by examining differences between Fourier amplitude spectra from paired recordings. As Fourier amplitude is assumed to be Gaussian their difference should be Gaussian. Empirical models of stochastic amplitude developed by Abrahamson (1992b, 2005) and Ancheta et al.

(2011) are based on the difference of log Fourier amplitudes from dense array recordings. The models express the standard deviation of the difference, $\sigma_{\Delta A}(\omega_n, \xi)$, as a function of frequency and separation distance. The standard deviation for stochastic amplitude at single station is not measureable, but can be estimated by scaling $\sigma_{\Delta A}(\omega_n, \xi)$ by $1/\sqrt{2}$. To create simulations over a 2D grid, the single station standard deviation function is translated into a covariance function as:

$$C_{\Delta A}(\omega_n, \xi) = \left(1/\sqrt{2}\, \sigma_{\Delta A}(\omega_n, \xi)\right)^2 \quad (12)$$

4. ANALYSIS-SYNTHESIS WINDOW SELECTION

In the STFT analysis and synthesis step, the short time segments of the signal are weighted with an appropriate analysis and synthesis window before they are transformed into the frequency domain. The requirements of an appropriate window are: (1) constant unity weighting of all time increments and (2) during the frequency domain convolution (as the analysis and synthesis requires time domain weighting), all sampled frequencies must fall on the window spectrum nulls. For brevity only the time domain requirement is discussed here while the frequency domain requirement is described by Ancheta (2010). The window tapers the beginning and end of the time series to prevent discontinuities during the Fourier transform. When time series are weighted or tapered some of the signal is lost. However, if the short time segments are overlapped the weighting within the overlapping section can be selected to add up to 1 (avoiding signal loss) by using an appropriate window.

We select a 2M+1 point Hamming window (modified from Harris, 1978):

$$w(t) = 0.54 + 0.45cos\left(\frac{\pi}{M}t\right) \quad (13)$$

The hop size for application of the Hamming window is (Smith, 2010):

$$R = 0.25(2M + 1) \quad (14)$$

where R is expressed as the number of time steps and M is related to window duration as:

$$M \approx L(2\Delta t) \quad (15)$$

where L is the window duration (e.g., Table 1) and Δt is the time step. Eq. (15) is exact if the right side is an odd number. Hop size R from Eq. (14) produces a 75% overlap of the short time segments. Within the 75% overlap region of the Hamming window, the sum of window weights is greater than one, which necessitates a down-scaling of the weights in Eq. (13). The window is used in both the analysis and synthesis, which effectively squares the weight applied by the window. Accordingly, after taking the square root, the window weights are divided by scaling factor F_w to create the overlap weighting equal to one:

$$F_w = 1.47 - \frac{1.888\Delta t}{L} \quad (16)$$

Available appropriate windows cannot be used without scaling as in Eq. (16) nor do they satisfy the frequency domain requirement perfectly, causing some degree of spectral leakage. Any selected windows must have their hop size and scaling factors determined separately. Eqs. (14-16) apply uniquely to the Hamming window with a 75% overlap.

5. ZERO PADDING

The STFT uses an overlapped but scaled window to ensure unity weighting for all overlapped time indices. However, non-overlapped time indices near the beginning and end of the time series will not be weighted to unity. Additionally, the short time segment at the end of the record is typically not a duration L. Therefore, zero padding is added in two phases:

1. Zero padding is added to the beginning and end of the time series before segmenting. Using a Hamming window with 75% overlap, the number of time steps in the zero padded zone is equal to the window length (2M+1).
2. Zero padding is added to the final segment (as needed) to increase its duration to L.

6. FIM SIMULATION

The Fourier Integral Method is referred to as a spectral simulation approach in that it utilizes the spectrum of the covariance function to generate a compatible spatially correlated random field. In this application the FIM is utilized to simulate the random fields of the noise Fourier amplitude and phase independently at each frequency. This section briefly discusses the FIM methodology adapted from Pardo-Iguzquiza and Chica-Olmo (1993). FIM utilizes the relationship between the stochastic process and its covariance function and their Fourier transforms.

Beginning with a stochastic process $z(u)$, the covariance function for a given frequency is:

$$C(\xi) = \frac{1}{N(\xi)} \sum_{\alpha=1}^{N(\xi)} z(u_\alpha) \cdot z(u_\alpha + \xi) - m_0 m_{+\xi}$$

(17)

where m_0 and $m_{+\xi}$ are the mean of the head and tail values,

$$m_0 = \frac{1}{N(\xi)} \sum_{\alpha=1}^{N(\xi)} z(u_\alpha)$$

$$m_{+\xi} = \frac{1}{N(\xi)} \sum_{\alpha=1}^{N(\xi)} z(u_\alpha + \xi)$$

and $N(\xi)$ is the number of pairs with a separation distance ξ. The Fourier transformation of $z(u)$ [with amplitude $|Z(\omega)|$ and phase, $\theta(\omega)$] is given by:

$$Z(\omega) = \int_{-\infty}^{\infty} z(u) e^{-i\omega u} du \qquad (18)$$

$$Z(\omega) = |Z(\omega)| e^{-i\theta(\omega)} \qquad (19)$$

Using the Wiener-Khintchine theorem the covariance is the Fourier transform of the stochastic process spectral density function, $S(\omega)$:

$$C(\xi) = \int_{-\pi}^{\pi} S(\omega) e^{i\omega\xi} d\omega \qquad (20)$$

Using the fact that the square of the unsmoothed Fourier amplitude is the spectral density function, the following steps will generate a stochastic process compatible with $z(u)$ starting from the covariance function:

1. Obtain the spectral density function by taking the Fourier transform of a covariance function.
2. Calculate the Fourier amplitude component of a Fourier series by taking the square root of the spectral density.
3. Add a random phase bounded between 0 and 2π to the Fourier amplitude component to create complex Fourier series.
4. Perform an inverse Fourier transform on the new series to produce a compatible stochastic process.

A number of implementation steps required including shifting and scaling of the covariance function, creating 2D hermitian Fourier components, and minimum length of field, are discussed in Pardo-Iguzquiza and Chica-Olmo (1993) and Yao (2004).

7. VALIDATION

In Figures 2a-c, we compare a seed motion (Fig 2a) to a single simulated motion in the time and frequency domains. The coherency and amplitude variability functions used in the procedure were taken from Ancheta et al. (2011). Figures 2b-c compare coherencies and amplitude variabilities derived from 25 simulated motions on a 25 m by 25 m grid with 5 meter spacing. To be consistent with the original models, the coherency and amplitude variability for the record pairs are calculated from the S-windows. Each dot in the amplitude variability figure (Figure 2b) represents the standard deviation of the log Fourier amplitude differences between unique pairs of the simulated motions (under the assumption that Fourier amplitudes are log-normal). Each dot in the coherency figure (Figure 2c) represents coherency between a station pair (in tanh[-1] space, where coherency is approximately normally distributed). The median values of the standard deviation and the coherency are compared to their median models.
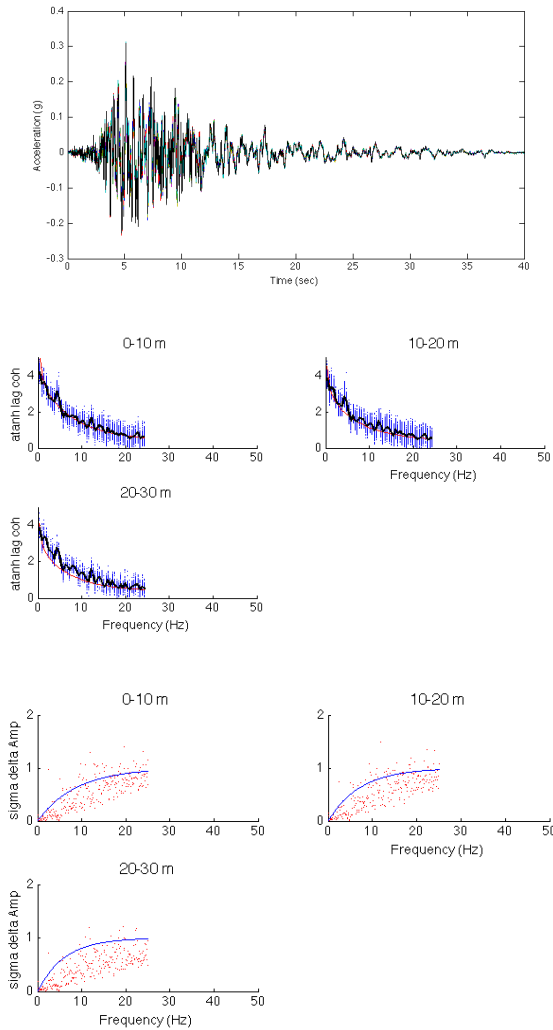
Figure 2a (top): Time series of input in black and 25 simulated stations in various colors. 2b(middle): Lagged coherency of simulated motions in blue dots and their median in solid black line compared to the target in solid red line. 2c(bottom): $\sigma_{\Delta A}$ of the simulated motions in red dots compared to the target in solid blue line.

The results in Figure 2a show that the simulations produce non-stationary ground motions with general characteristics similar to those of the seed record. There are no frequency bands where the simulated Fourier amplitudes are biased from the seed (indicating minimal spectral aliasing). Figure 2b shows that mean lagged coherencies of the simulations (comparing all possible record pairs) are practically unbiased relative to the target model. Figure 2c shows that amplitude variability is

under-predicted, which results from removal of segment means (details in Ancheta, 2010). If these means were not removed, the $\sigma_{\Delta A}$ terms would match the target model, but at the expense of simulated waveforms in which some time increments have unrealistically rich high frequency energy.

8. CONCLUSIONS

We present a methodology for conditional simulation of spatially variable ground motion in a 2D plane. The method takes as input user-specified functions for Fourier amplitude variability and coherency, along with a seed record. The method produces spatially variable ground motions that in aggregate match the characteristics of the target functions while maintaining the non-stationary characteristics of the seed record.

Implementation details that remain under development pertain to (1) selection of segment duration and frequency bands that improve the analysis and synthesis window and (2) improved fit of the target amplitude variability model.

9. ACKNOWLEDGMENTS

10. REFERENCES

Abrahamson, NA, 1992a, Generation of spatially incoherent strong motion time histories, *Proc. 10th World Conf. Earthquake Eng.*, 845-850.

Abrahamson, N.A. 1992b, "Spatial variation of earthquake ground motion for application to

soil-structure interaction," Electrical Power Research Institute, Rpt. No. EPRI TR-100463

Abrahamson, NA, 2005, Effect of local site condition on spatial coherency, *Rpt. No.RP2978-05*, Electric Power Research Institute, Palo Alto, CA.

Allen, JB and LR Rabiner, 1977, A unified approach to short-time Fourier analysis and synthesis, *Proc. IEEE*, **65** (11), 1558-1564.

Ancheta, T.D. Stewart, J.P., Abrahamson, N.A., 2011, "Engineering characterization of earthquake ground motion coherency and amplitude variability," Proc. 4th IASPEI/IAEE Int. Sym. On Effects of Surface Geology on Seismic Motion, University of Santa Barbara, August 23-26, 2011.

Ancheta, T.D., 2010, Engineering Characterization of Spatially Variable Earthquake Ground Motions, Phd Dissertation, UCLA.

Boissieres, H-P and EH Vanmarcke, 1995, Estimation of lags for a seismograph array: wave propagation and composite correlation, *Soil Dyn. Eqk. Eng*, **14**, 5-22.

Hao, H, CS Oliveira, and J Penzien, 1989, Multiple-station ground motion processing and simulation based on SMART-1 array data, *Nucl. Eng. Des*., **111**, 293-310.

Harris, FJ, 1978, On the use of windows for harmonic analysis with the discrete Fourier transform, *Proc. IEEE*, **66** (1), 51-83.

Harichandran, RS and EH Vanmarcke, 1986, Stochastic variation of earthquake ground motion in space and time, *J. Eng. Mech. Div.*, **112**, 154-174.

Luco, JE and HL Wong, 1986, Response of a rigid foundation to a spatially random ground motion, *Earthquake Engin. Struct. Dyn.*, **14**, 891-908.

Pardo-Iguzquiza, E., and Chica-Olmo, M., 1993, The Fourier integral method: An efficient spectralmethod for simulation of random fields: Math. Geol., v. 25, no. 4, p. 177–217.

Serra, X., Smith, J. O., 1990, Spectral Modeling Synthesis: A Sound Analysis/Synthesis System Based on a Deterministic Plus Stochastic Decomposition, Computer Music Journal, Vol. 14, No. 4 (Winter, 1990), pp. 12-24

Smith, J. O., 2010 draft, Spectral Audio Signal Processing, http://ccrma.stanford.edu/~jos/sasp/, online book.

Vanmarcke, EH, E Heredia-Zavoni, and GA Fenton, 1993, Conditional simulation of spatially correlated earthquake ground motion, *J. of Eng. Mech.* **119**, 2333-2352.

Vanmarcke E. and G. Fenton, 1991, "Conditioned Simulation of Local Fields of Earthquake Ground Motion", Structural Safety, 10, 247-264.

Yao, T., 2004, Reproduction of the Mean, Variance, and Variogram Model in Spectral Simulation. Math. Geol., v. 36, no. 4, p. 487–506.

Zerva, A., 2009, *Spatial Variation of Seismic Ground Motions: Modeling and Engineering Applications*, CRC Press, Florida.

Zerva, A., and Zervas, V., 2002, "Spatial variation of seismic ground motions: An overview," Appl Mech Rev, 55, No. 3, ASME Reprint No AMR 328, 271-297.